

Supplemental Information Schäfer et al.:

## **Impaired DNA demethylation of C/EBP sites causes premature aging**

### **Inventory**

#### Supplemental Figures

Figure S1, related to Figure 1

Figure S2, related to Figure 2 and 3

Figure S3, related to Figure 4

Figure S4, related to Figure 5

Figure S5, related to Figure 6

Figure S6, related to Figure 7

#### Supplemental Tables

Supplemental Table S1, spreadsheet, related to Figure 2  
DMR list of whole genome bisulfite sequencing

Supplemental Table S2, spreadsheet, related to Figure 3  
GADD45 $\alpha$  ChIP-Seq peaks

Supplemental Table S3, spreadsheet, related to Figure 4  
Ing1 ChIP-Seq peaks

Supplemental Table S4, spreadsheet, related to Figure 4  
RNA-Seq in undifferentiated MEFs

Supplemental Table S5, spreadsheet, related to Figure 4  
NG-Capture C viewpoints

Supplemental Table S6, spreadsheet, related to Figure 5  
RNA-Seq at day 6 of MEF adipocyte differentiation

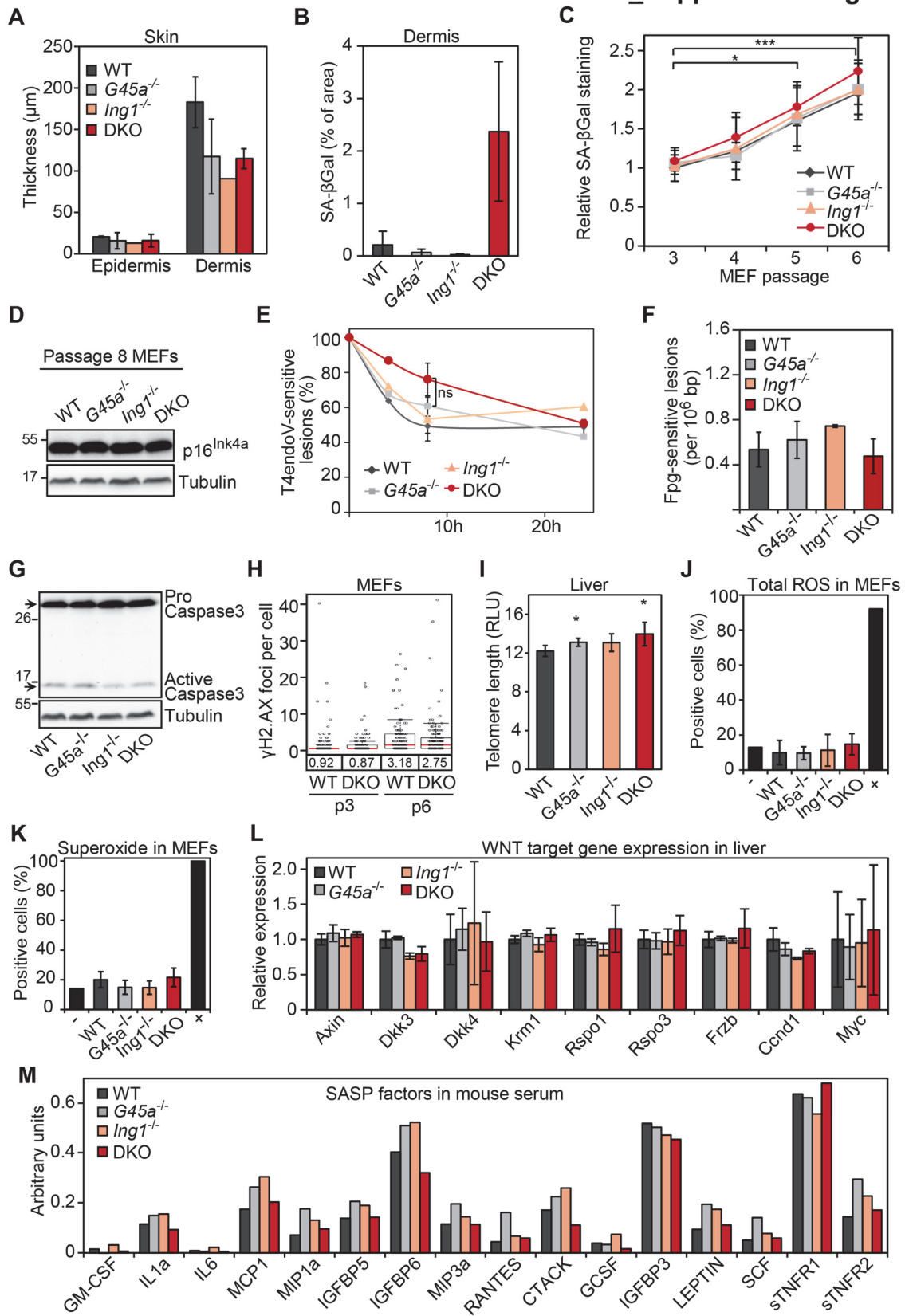
Supplemental Table S7, spreadsheet, related to Figure 6  
Microarray of white adipose tissue

Supplemental Table S8, related to Figure 7 and S7

#### Supplemental primer sequences

#### Supplemental references

Schäfer\_Supplemental Fig. S1



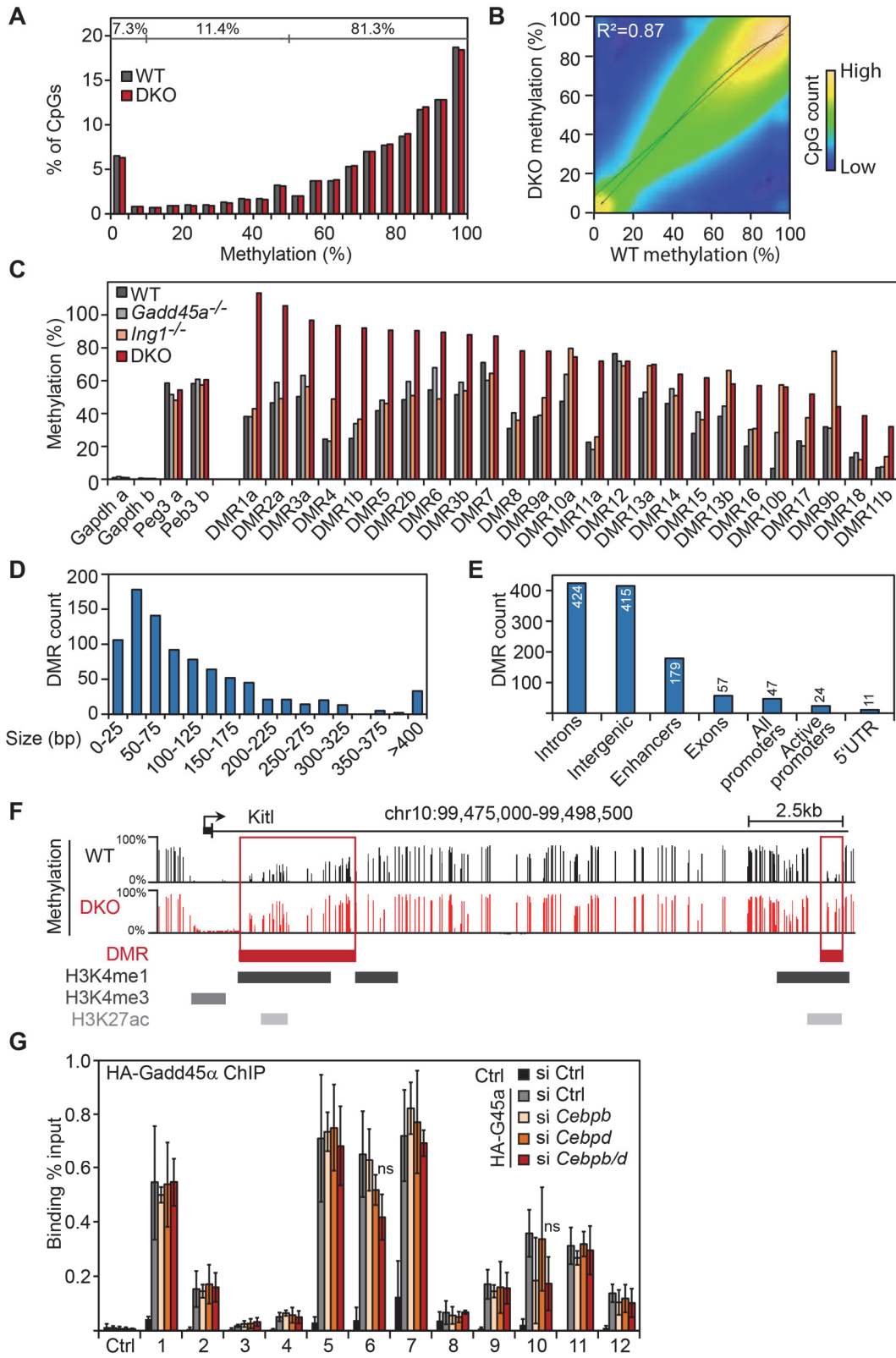
## Supplemental Figure S1 | Loss of *Gadd45a* and *Ing1* promotes segmental progeria

- (A) Quantification of epidermal and dermal thickness in H&E-stained sections of hind limb skin from Fig. 1D. n=1-4 mice per genotype.
- (B) Quantification of senescence-associated  $\beta$ -Galactosidase (SA- $\beta$ Gal) staining in mouse dermis from Fig. 1E; n=5 animals per genotype.
- (C) Senescence-associated  $\beta$ -Galactosidase (SA- $\beta$ Gal) assay in MEFs at indicated passages. n=3 independent cell lines per genotype.
- (D) Immunoblot of the senescence marker p16INK4a in passage 6 MEFs of indicated genotypes.  $\alpha$ -Tubulin served as loading control. n=3 independent MEF lines per genotype
- (E) Repair kinetics of T4-endonuclease V-sensitive cyclobutane pyrimidine dimers (CPDs) in passage 4 MEFs was determined at 4h, 8h and 24h after UVB treatment to monitor cellular NER capacity. n= 3 for the 8h data point. At 8h, there was no change in *Ing1*<sup>-/-</sup> MEFs vs WT, but a significant change in *Gadd45a*<sup>-/-</sup> (p=0.03) and DKO- (p=0.003) vs WT MEFs. The difference between DKOs vs *Gadd45a*<sup>-</sup> or vs *Ing1* single mutants was statistically not significant.
- (F) Fpg (formamidopyrimidine - DNA glycosylase) -sensitive oxidized purines and AP sites, reflecting cellular BER capacity, were determined in passage 4 MEFs in steady-state. n=3
- (G) Immunoblot of apoptosis marker Caspase 3 in passage 6 mouse embryonic fibroblasts (MEFs) of indicated genotypes.  $\alpha$ -Tubulin was used as loading control. Molecular weight of proteins in kDa is indicated on the left. WT, wildtype; DKO, *Gadd45a/Ing1* double knockout
- (H) Quantification of  $\gamma$ H2A.X staining of WT and DKO MEFs at passages 3 (p3) and 6 (p6) to analyze DNA damage accumulation. n>100 cells per condition and genotype were quantified. Dots indicate numbers of foci in individual cells, red lines indicate median values, whiskers of the box plot represent data within 1.5x interquartile range. Numbers below the box plots indicate average number of  $\gamma$ H2A.X foci per cell.
- (I) Telomere length in mouse livers of indicated genotype (n=4 per genotype) measured by Southern Blot analysis. RLU, relative length units
- (J-K) Quantification of total reactive oxygen species (ROS) (J) and superoxide (K) levels by flow cytometry in passage 3 MEFs (n=4 individual lines per genotype). An N-Acetyl-Cysteine treated negative control (-) and a Pyocyanine-treated positive control (+) served as calibration references.
- (L) Gene expression analysis of WNT target genes as an indicator of stem cell function in mouse livers (n=9 per genotype).
- (M) Protein levels of senescence-associated secretory phenotype (SASP) related cytokines measured by a cytokine protein array in mouse serum (three pooled serum samples per genotype). Signal intensities are only comparable within analysis of the same protein.

Data of bar charts represent mean values of the indicated number of samples +/- SD.

\*, p<0.05; \*\*\*, p<0.001. G45a, *Gadd45a*

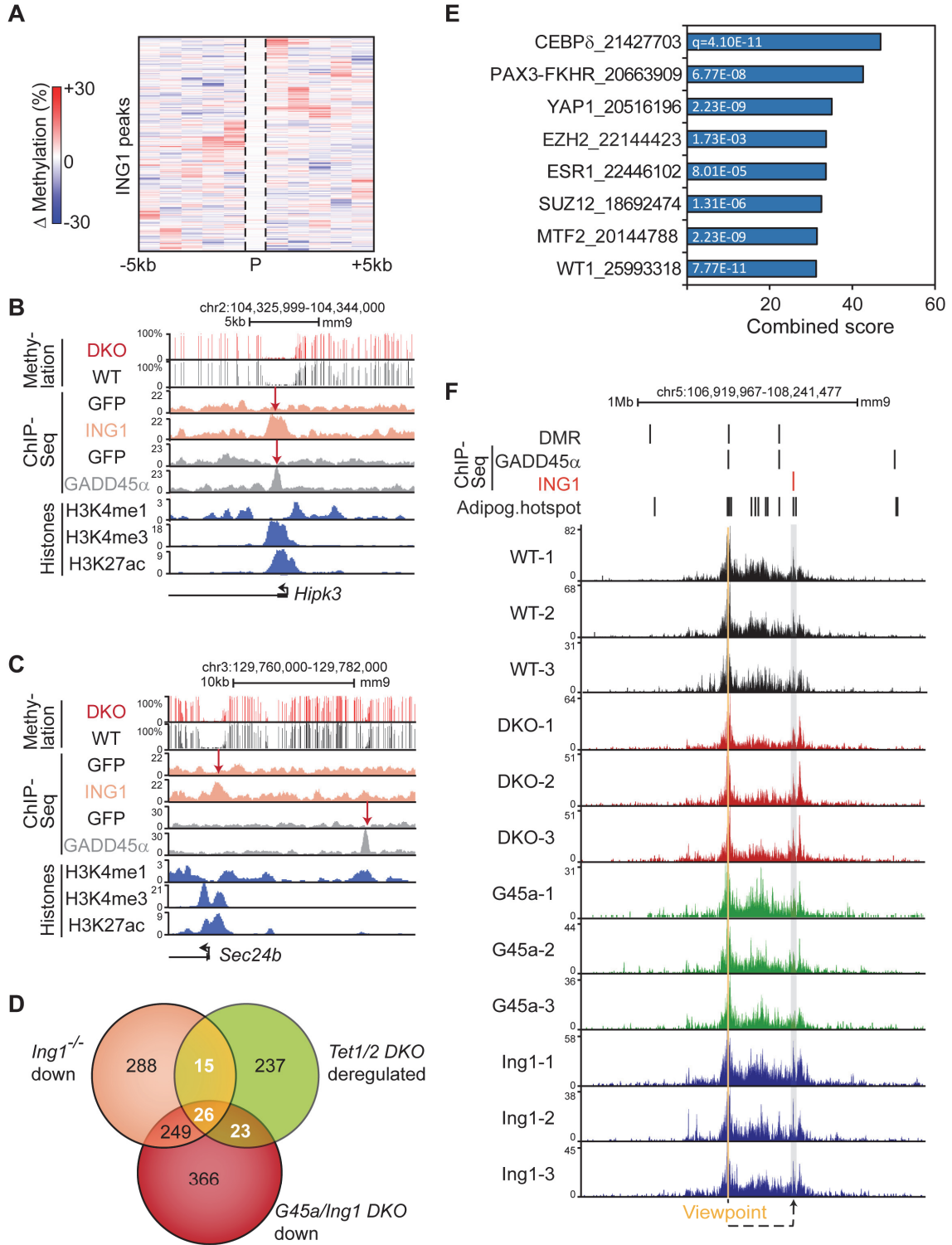
Schäfer\_Supplemental Fig. S2



## Supplemental Figure S2 | Whole-genome bisulfite sequencing reveals local DNA hypermethylation in *Gadd45a/Ing1* DKO-MEFs

- (A) Histogram of distribution of DNA methylation levels measured by Whole-genome bisulfite sequencing (WGBS) in wildtype (WT) and *Gadd45a/Ing1* double-knockout (DKO) MEF lines.
- (B) Genome-wide correlation of DNA methylation levels at individual CpGs in WT and DKO MEF lines.
- (C) Confirmation of hypermethylated DMRs. Methylation-sensitive qPCR measurements of (5mC+5hmC) levels at CpGs within the unmethylated *Gapdh* promoter, the imprinted *Peg3* locus, and several hypermethylated differentially methylated regions (DMRs) in MEFs of the indicated genotypes.
- (D) Histogram showing size distribution of hypermethylated DMRs of DKO MEFs.
- (E) Genomic locations of DKO hypermethylated DMRs. Numbers indicate absolute numbers of DMRs within each category. DMRs that fall within more than one category were counted in each category. Active promoters are defined as regions  $\pm$  1 kb of transcription start site (TSS) decorated by H3K4me3. Enhancers are defined as regions decorated by both H3K4me1 and H3K27ac.
- (F) Exemplary DMR at the *Kitl* gene in WT vs. DKO MEFs. Methylation at individual CpGs as measured by WGBS; MEF histone marks are from (Yue et al. 2014).
- (G) GADD45 $\alpha$ -ChIP-qPCR. MEFs were transiently transfected with either control or *Cebpb*- and/or *Cebpd*- specific siRNA, followed by transient *HA-Gadd45a*- (HA-G45a) or control- (Ctrl) transfection. GADD45 $\alpha$  binding to 12 genomic regions identified in the ChIP-Sequencing was analysed. An unrelated control region served as negative control (Ctrl). Data represent the mean of biological triplicates  $\pm$  SD. *Cebpb* and *Cebpd* knockdown was controlled by qPCR and greater than 80% or 50%, respectively (data not shown). ns, not significant

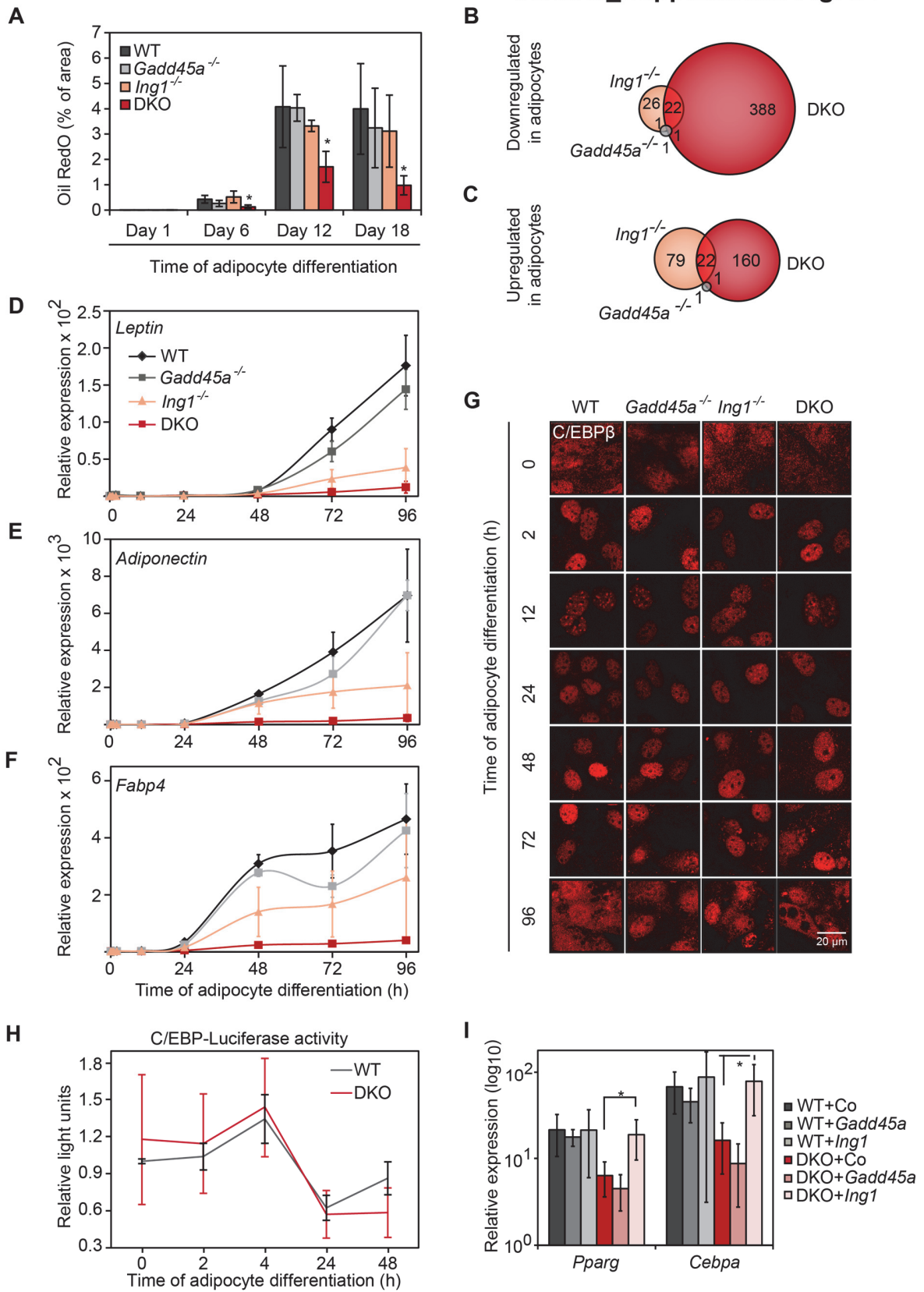
### Schäfer\_Supplemental Fig. S3



### Supplemental Figure S3 | ING1 binds to hypomethylated promoters and can loop to GADD45 $\alpha$ sites

- (A) Heatmap of mean differential methylation in 1kb bins around ING1 ChIP-Seq peaks (P). Data are presented as DNA methylation difference between DKO MEFs and WT MEFs as determined by WGBS.
- (B-C) Exemplary genomic loci showing GADD45 $\alpha$  and ING1 occupancy in WT and DKO MEFs. Methylation at individual CpGs as measured by WGBS, ChIP-Seq profiles of transfected HA-tagged ING1 and GADD45 $\alpha$  in MEFs with their respective GFP control from this study; MEF histone marks from (Yue et al. 2014). (B) Example of overlapping GADD45 $\alpha$  and ING1 ChIP-Seq peaks around the TSS of the *Hipk3* gene. (C) Example of an enhancer-associated GADD45 $\alpha$  peak in vicinity of a promoter-associated ING1 peak at the *Sec24b* gene.
- (D) Overlap between *Tet1/2* DKO deregulated genes (Wiehle et al. 2015) and  $\geq 1.5$ -fold-downregulated genes in *Ing1*<sup>-/-</sup> or DKO MEF.
- (E) Genes hypermethylated and downregulated in DKOs MEFs are enriched for C/EBP $\delta$  motifs. Hypermethylated DMR-associated genes from *Ing1/Gadd45a* DKO MEFs (n=1331, closest genes determined by analysis with GREAT, <http://great.stanford.edu/public/html/>) were intersected with genes downregulated in DKO MEFs (n=966 with log<sub>2</sub> fold-change < -0.35 at 10% FDR). Overlapping genes were subjected to geneset enrichment analysis of transcription factor targets from the ChIP-X database (ChEA 2016-Enrichr <http://amp.pharm.mssm.edu/Enrichr>). Enriched transcription factors are displayed on the Y-axis along with PMIDs of the original studies. The combined score represents the enrichment and is calculated by Enrichr from p-value (Fisher exact test) and the z-score of the deviation from the expected rank. Adjusted p-value (q) is indicated in the bar chart. Note that downregulated genes are highly enriched for C/EBP $\delta$  binding sites.
- (F) Top, GADD45 $\alpha$ - and ING1-ChIP-seq peaks, hypermethylated DMRs identified in *Gadd45a/Ing1* double knockout (DKO) MEFs, and adipogenic hotspots (based on (Siersbaek et al. 2014)). Bottom, NG-Capture C interaction profile of all wildtype (WT), *Gadd45a*<sup>-/-</sup> (G45a), *Ing1*<sup>-/-</sup> (Ing1) and DKO MEF lines in triplicates in a 1.3Mb genomic region on chromosome 5. The interaction between the GADD45 $\alpha$ -bound viewpoint (orange) with the *Tgfbr3* promoter bound by ING1 is highlighted (grey shading). Replicate 2 of WT and of DKO are shown in Fig. 4H.

Schäfer\_Supplemental Fig. S4

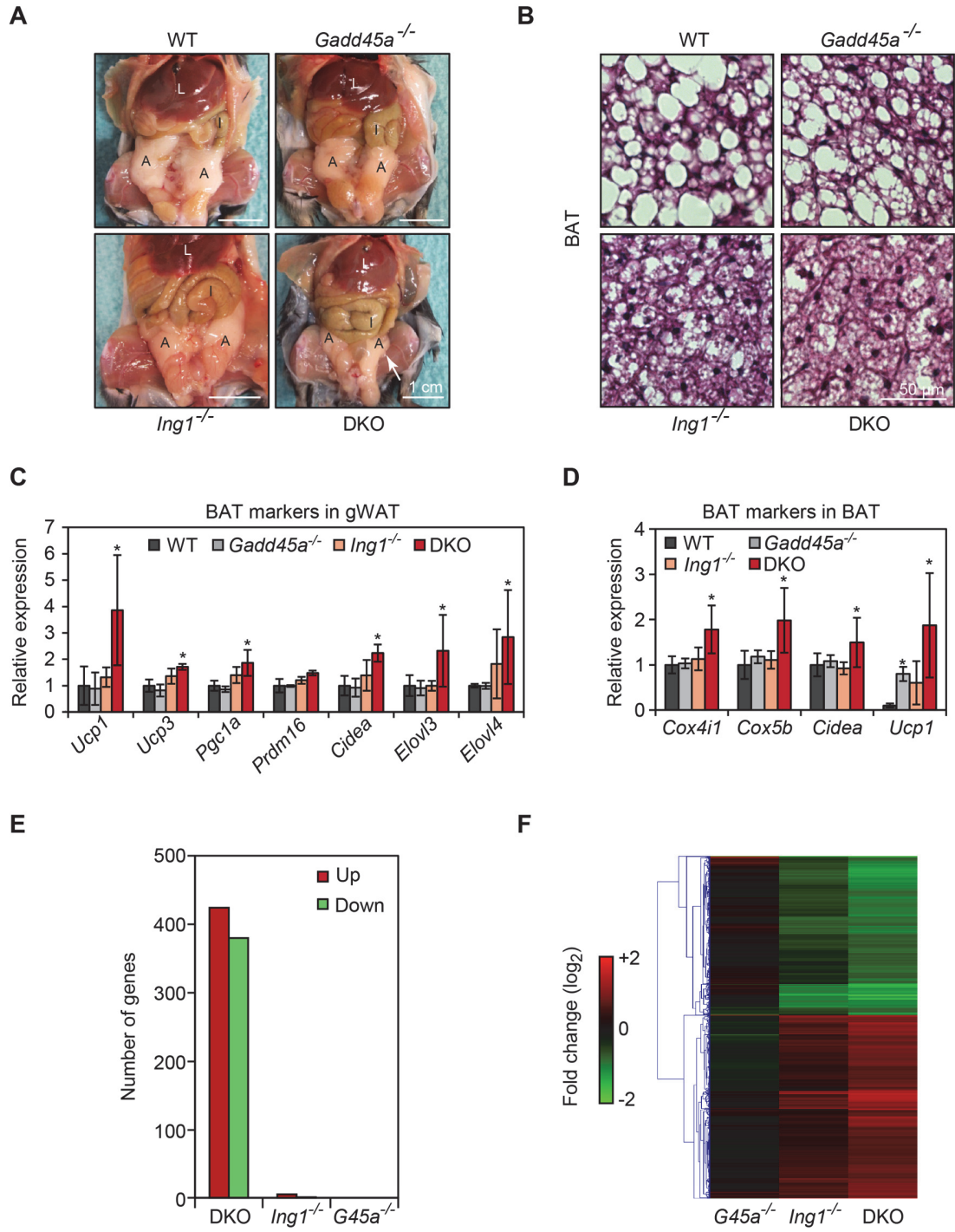




### Supplemental Figure S4 | *GADD45a* and *ING1* are required for adipocyte differentiation downstream of *C/EBPβ*

- (A) Quantification of Fig. 5b. Areas with positive staining for Oil Red O were quantified in 9 overview micrographs per MEF line and time point. \*,  $p < 0.05$  compared to wildtype (WT) at same time point.
- (B-C) Transcriptome analysis in differentiating MEFs. RNA-seq analysis at day six of MEF-to-adipocyte differentiation showing overlap of  $\geq 2$ -fold downregulated (B) or upregulated (C) genes at 10% FDR in indicated genotypes compared to WT. Values indicate numbers of deregulated genes in the respective genotype.
- (D-F) qPCR expression analysis of late adipogenic marker genes *Leptin* (D), *Adiponectin* (E) and *Fabp4* (F) during MEF-to-adipocyte differentiation in indicated genotypes. Data are presented as mean values of three independent MEF lines per genotype +/- SD.
- (G) Immunofluorescence microscopy of endogenous *C/EBPβ* during MEF-to-adipocyte differentiation in indicated genotypes and time points. Note the translocation to the nucleus at 2h and foci formation at 12h, which are unaltered in DKO.
- (H) Luciferase reporter assay for a *C/EBP*-responsive reporter transiently overexpressed in WT and DKO cells during MEF-to-adipocyte differentiation. Data are presented as mean values of three independent MEF lines per genotype +/- SD.
- (I) *Gadd45a* or *Ing1* was transfected in WT and DKO MEFs and differentiated to adipocytes for four days. Expression of the adipogenic marker genes *Pparg* and *Cebpa* was measured by qPCR. Data are represented as mean values of three independent MEF lines +/- SD. p-value shown for most relevant expression changes. \*,  $p < 0.05$

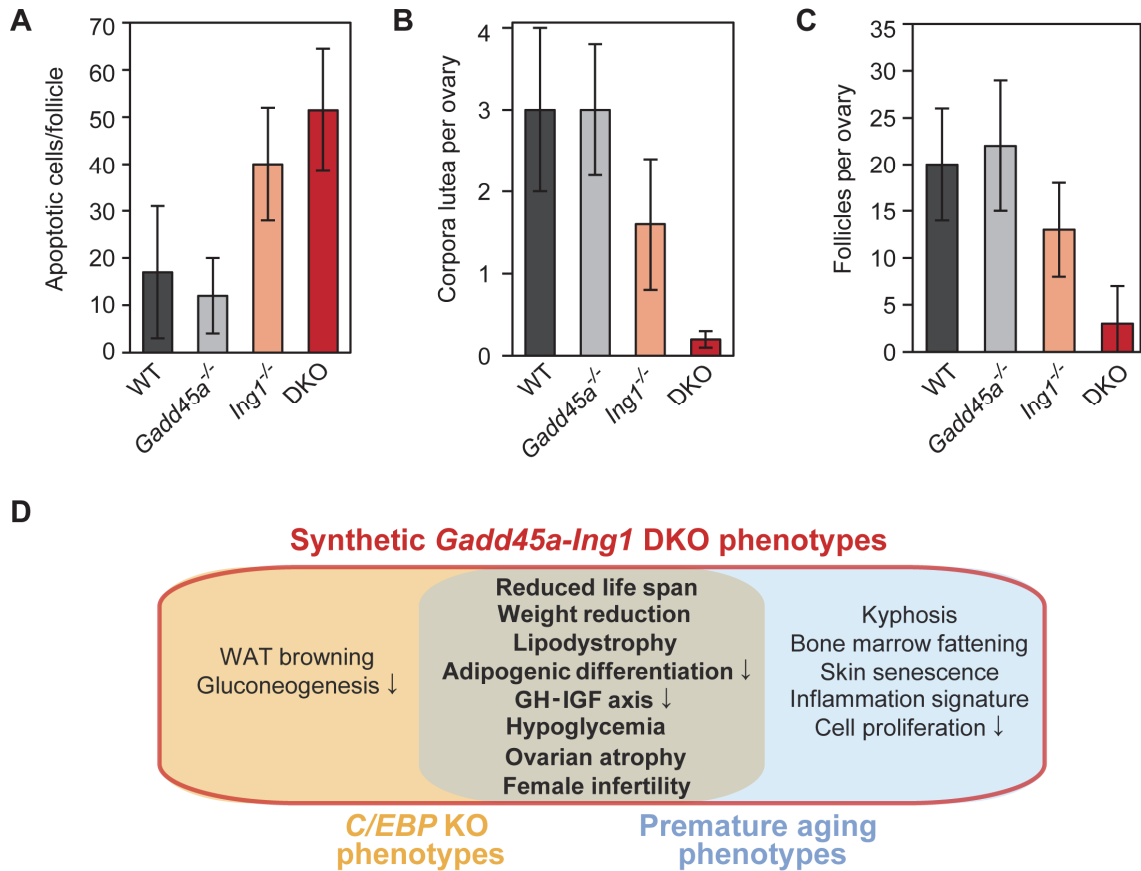
Schäfer\_Supplemental Fig. S5



## Supplemental Figure S5 | Synthetic lipodystrophy in *Gadd45a/Ing1* DKO mice

- (A) *In situ* overview of mouse abdominal cavities of representative animals for each genotype. L, liver; I, intestines; A, gonadal white adipose tissue (gWAT). The white arrow points to reduced gWAT depots of the *Gadd45a/Ing1* double knockout (DKO) mouse. WT, wildtype
- (B) Histological image (H&E stain) of interscapular brown adipose tissue (BAT). Representative images from n=3-6 animals per genotype.
- (C) qPCR expression analysis of brown adipose tissue (BAT) related genes in gonadal white adipose tissue (gWAT) (n=5-9 mice per genotype).
- (D) qPCR expression analysis of brown adipose tissue (BAT) related genes in BAT (n=3-5 mice per genotype).
- (E-F) Transcriptome analysis in WAT. Microarray expression analysis was performed on gWAT from three pools of three mice each per genotype. (E) Bar chart showing the number of  $\geq 1.5$ -fold up- and downregulated genes at 10% FDR, respectively, in indicated genotypes compared to WT. No genes were significantly up- or downregulated in *Gadd45a*<sup>-/-</sup> mice. (F) Heatmap of  $\geq 1.5$ -fold down- (green) and upregulated (red) genes in DKO gWAT at FDR 10%. Note that most of the expression changes in *Ing1*<sup>-/-</sup> single mutants, visible in (F), are not statistically significant (see bar chart in (E)).

## Schäfer\_Supplemental Fig. S6



### Supplemental Figure S6 | GADD45α/ING1 promote C/EBP function and impact aging

(A-C) Quantification of apoptotic cells per follicle (A), corpora lutea per ovary (B), and follicles per ovary (C) in H&E stained ovary sections of indicated genotypes (Fig. 7E). Data are presented as mean values of n=5 animals per genotype +/- SD.

(D) Overlap of synthetic phenotypes of *Gadd45a*/*Ing1* DKO mice with phenotypes exhibited by mice mutant for *Cebp* and progeroid mice, respectively (see also Supplemental Table S8).

**Supplemental Tables S1-S7 as spreadsheets**

**Supplemental Table S8:** Occurrence of symptoms associated with aging in < 2 months old *Gadd45a-Ing1* double-knockout (DKO) and *C/EBP* KO mice.

Symptom	Occurrence in <i>Gadd45a-Ing1</i> DKO mice	Occurrence in <i>C/EBP</i> KO mice	Occurrence in prematurely aging mice
Weight reduction	yes	Rahman et al. 2012; Staiger et al. 2009; Wang et al. 1995	Andressoo et al. 2009; de Boer et al. 1998; Harada et al. 1999; Mounkes et al. 2003; Niedernhofer et al. 2006; Pendas et al. 2002; Trifunovic et al. 2004; van de Ven et al. 2006; van der Pluijm et al. 2007
Lipodystrophy	yes	Rahman et al. 2012; Staiger et al. 2009; Tanaka et al. 1997; Wang et al. 1995	de Boer et al. 1998; Hemmeryckx et al. 2012; Karakasilioti et al. 2013; Peinado et al. 2011; Pendas et al. 2002; Trifunovic et al. 2004; van der Pluijm et al. 2007
Decreased adipogenic differentiation	yes	Tanaka et al. 1997	Compe et al. 2005
Dampened GH-IGF1 axis	yes	Arizmendi et al. 1999; Rahman et al. 2012; Staiger et al. 2009	Niedernhofer et al. 2006; van de Ven et al. 2006; van der Pluijm et al. 2007
Hypoglycemia	Yes	Arizmendi et al. 1999; Liu et al. 1999; Rahman et al. 2012; Wang et al. 1995	Niedernhofer et al. 2006; van de Ven et al. 2006
Ovarian atrophy	yes	Sterneck et al. 1997	de Boer et al. 2002; Kuro-o et al. 1997
Female infertility	yes	Sterneck et al. 1997; Tanaka et al. 1997	de Boer et al. 1998; Kuro-o et al. 1997; Trifunovic et al. 2004
Perinatal death (partial penetrance) *	yes	Tanaka et al. 1997	van der Pluijm et al. 2007
Reduced life-span	yes	Screpanti et al. 1995	Andressoo et al. 2009; de Boer et al. 1998; Harada et al. 1999; Kuro-o et al. 1997; Mounkes et al. 2003; Niedernhofer et al. 2006; Trifunovic et al. 2004; van de Ven et al. 2006; van der Pluijm et al. 2007; Vogel et al. 1999

Inflammation-signature	yes	Huggins et al. 2013	Karakasilioti et al. 2013; Lumeng et al. 2011
WAT browning	yes	Rahman et al. 2012	
Reduced gluconeogenesis	yes	Arizmendi et al. 1999; Inoue et al. 2004; Liu et al. 1999; Wang et al. 1995	
Small body size	yes		Andressoo et al. 2009; Harada et al. 1999; Kuro-o et al. 1997; McWhir et al. 1993; Mounkes et al. 2003; Niedernhofer et al. 2006; Pendas et al. 2002; van de Ven et al. 2006; van der Pluijm et al. 2007; Vogel et al. 1999
Kyphosis	yes		Andressoo et al. 2009; de Boer et al. 2002; Kuro-o et al. 1997; Niedernhofer et al. 2006; Pendas et al. 2002; Trifunovic et al. 2004; van de Ven et al. 2006; van der Pluijm et al. 2007; Vogel et al. 1999
Bone marrow fattening	yes		Moore and Dawson 1990; Prasher et al. 2005
Skin senescence	yes		Dimri et al. 1995; Kuro-o et al. 1997
Decreased cell proliferation	yes		Mounkes et al. 2003; Niedernhofer et al. 2006
Decreased bone density	n.d.	Smink et al. 2009	Brennan et al. 2014; Chen et al. 2013
Increased apoptosis	n.d.		Harada et al. 1999
Increased DNA double strand breaks	n.d.		White et al. 2015
Telomere shortening	n.d.		Jaskelioff et al. 2011; Rudolph et al. 1999
Increased ROS production	n.d.		
Change in WNT signaling	n.d.		Brack et al. 2007; Castilho et al. 2009; Liu et al. 2007
Increased circulating senescence-associated factors	n.d.		Coppe et al. 2008; Coppe et al. 2010

**Comments:**

\* Not mentioned in the manuscript

n.d. No difference

## Supplemental Material and Methods

### Primer sequences: qRT-PCR primers

Target	Forward primer sequence	Reverse primer sequence	UPL probe
<i>Acadl</i>	TGGGGACTTGCTCTCAACA	GGCCTGTGCAATTGGAGTA	103
<i>Acadm</i>	AGTACCCTGTGGAGAAGCTGAT	TCAATGTGCTCACGAGCTATG	110
<i>Acadsb</i>	TCCAGATAGGGAAACGAGAAAA	TCCCCAAAATATTAGTCTCTGGAA	105
<i>Adiponectin</i>	GGAGAGAAAGGAGATGCAGGT	CTTTCCTGCCAGGGGTTTC	17
<i>Aldh2</i>	TGTTTCGGGGACGTAAAAGAC	TGAGGATTTGCATCACTGGT	63
<i>Cebpa</i>	AAACAACGCAACGTGGAGA	GCGGTCATTGTCACCTGGTC	67
<i>Cebpb</i>	TGATGCAATCCGGATCAA	CACGTGTGTTGCGTCAGTC	102
<i>Cebpd</i>	CTTTTAGGTGGTTGCCGAAG	GCAACGAGGAATCAAGTTTCA	33
<i>Cidea</i>	TTCAAGGCCGTGTTAAGGA	CCTTTGGTGCTAGGCTTGG	46
<i>Cox4i</i>	TCACATGCGCTCGTTCTGAT	CGATCGAAAGTATGAGGGATG	7
<i>Cox5b</i>	TCCCATGGCTTCGGAGGT	GCCTTTGGAGGTAGCATATTGT	26
<i>Cyt c</i>	AACGTTTCGTGGTGTGACC	TTATGCTTGCCTCCCTTTTC	104
<i>Dhrs4</i>	GAGTGTGACTGGCATCGTGT	ATATCAATCCCCTGGTGACG	60
<i>Elovl3</i>	ACTTCGAGACGTTTTCAGGACTTA	GACGACCACTATGAGAAATGAGC	25
<i>Elovl4</i>	ACGACACCGTGGAGTTCTATC	GCGGCCAGTCTGCTACAC	85
<i>Fabp4</i>	AAGAGAAAACGAGATGGTGACAA	CTTGTGGAAGTCACGCCTTT	31
<i>G6pc</i>	TCTGTCCGGATCTACCTTG	GAAAGTTTCAGCCACAGCAA	19
<i>Gadd45a</i>	GCTGCCAGCTGCTCAAC	TCGTGCTCTTCGTCAGCA	98
<i>Gapdh</i>	AGCTTGTCAACACGGGAAG	TTTGATGTTAGTGGGGTCTCG	9
<i>Idh3b</i>	GCTGCGGCATCTCAATCT	CCATGTCTCGAGTCCGTACC	67
<i>Igf1</i>	CTGCTTGCTCACCTTCACC	AGCCTGTGGGCTTGTGTA	22
<i>Ing1</i>	CCTCCTTCTTCGTGCAGATTG	TCTGGCGTTTGAACCTGTCATAG	17
<i>InsR</i>	GAGAATTTCCCTTACAATTCCATC	CACTTGCATGACGTCTCTCC	104
<i>Irs1</i>	CTATGCCAGCATCAGCTTCC	TTGCTGAGGTCATTTAGGTCTTC	71
<i>Leptin</i>	CAGGATCAATGACATTTACACA	GCTGGTGAGGACCTGTTGAT	93
<i>Ndufab1</i>	TGCAGATAAGAAGGATGTGTATGAA	CTGTCACTCGGCCACGAT	109
<i>Ndufv1</i>	GGGTGAGATGAAGACATCAGG	TCAGCATTACCACCAGATACT	60
<i>Pepck</i>	GGAGTACCCATTGAGGGTATCAT	GCTGAGGGCTTCATAGACAAG	49
<i>Pex19</i>	TGCTGTACCCATCCCTGAA	GGAGGAGTGGAGTCCTGGT	50
<i>Pex3</i>	CAATGTGGAATTTCTGAAACG	TCTGTCCATATTTCCAGGAT	104
<i>Pgc1a</i>	GAAAGGGCCAAAACAGAGAGA	GTAAATCACACGGCGCTCTT	29
<i>Plin1</i>	AACGTGGTAGACACTGTGGTACA	TCTCGGAATTCGCTCTCG	64
<i>Ppara</i>	CACGCATGTGAAGGCTGTAA	GCTCCGATCACACTTGTGCG	41
<i>Pparg</i>	CAAGCCCTTTACCACAGTTGA	CAGGTTCTACTTTGATCGCACTT	67
<i>Prdm16</i>	TCTCGATCCCATCCTCA	GGAAGATCTTGCCACAGTACCT	12
<i>Thp</i>	GGGGAGCTGTGATGTGAAGT	CCAGGAAATAATTCTGGCTCA	97
<i>Ucp1</i>	GGCCTCTACGACTCAGTCCA	TAAGCCGGCTGAGATCTTGT	34
<i>Ucp3</i>	TACCCAACCTTGGCTAGACG	GTCCGAGGAGAGAGCTTGC	69
<i>Axin2</i>	GAGAGTGAGCGGCAGAGC	CGGCTGACTCGTTCTCCT	96
<i>Dkk3</i>	GCCTGAAGGAGCTTTGGAC	GGCTTGCACATGTACACCAG	76
<i>Dkk4</i>	ACGAAGAAATCACAAGCAGTAAG	AAAAATGGCGAGCACAGC	81
<i>Kremen1</i>	CCCCAGGTAGCCATTCCCT	CAGGCCGTACACAGTCCA	5
<i>Rspo1</i>	CGACATGAACAAATGCATCA	CTCCTGACACTTGGTGCAGA	5
<i>Rspo3</i>	TCAAAGGGAGAGCGAGGA	CAGAGGAGGAGCTTGTTTCC	103
<i>Frzb</i>	CACCGTCAATCTTTATACCACCT	TCAGCTATAGAGCCTTCTACCAAGA	34
<i>Ccnd1</i>	TTTCTTCCAGAGTCATCAAGTGT	TGACTCCAGAAGGGCTTCAA	72
<i>Myc</i>	CCTAGTGCTGCATGAGGAGAC	TCCACAGACACCACATCAATTT	77

## ChIP-qPCR primers (Fig. 2I and Fig. 6F)

Note: Primers are not identical with Supplemental Fig. S2C

Primer	Genomic coordinates (NCBI37/mm9)	Primer sequence (forward and reverse)	UPL probe
<b>CTRL1</b> (Gapdh)	chr6:125115169-125115257	f: CCTACGCAGGTCTTGCTGA r: TGACCTTGAGGTCTCCTTGG	10
<b>CTRL2</b>	chrX:83550052-83550147	f: CAGTTGGAAAGTCTCAGAGAGTAGAG r: TGTGGTGGTATGGGTGCTC	48
<b>DMR1</b>	chr4:97771169-97771233	f: CACTGCAGGAGGCCAAAC r: TGGGTCTCCATAGCACAGC	107
<b>DMR2</b>	chr5:107420642+107420733	f: ACCTTGGTGCCTCCATAAAGA r: CACTGCGGTGAGGAGAGAGT	SYBR
<b>DMR3</b>	chr17:50250575+50250654	f: AACATTCTGCAGCCCATTTT r: ACAACCAGGGCATTGCTTA	6
<b>DMR4</b>	chr4:80955790+80955906	f: GCAAGAGAGCTGATCCCGTA r: TGACATCACCTCCCTCCTTT	SYBR
<b>DMR5</b>	chr12:76803394+76803467	f: CTGGAGCCGTTTCTTCAGG r: ATTTTGTGGTGGGCTTCTTA	62
<b>DMR6</b>	chr1:170292711-170292778	f: GGGACAGGGAGCTACTAGGAA r: TCGCACTTGGCAAGACTCTA	67
<b>DMR7</b>	chr5:107420675-107420749	f: GATAATCCAAACAAAGCTAAGAATGTT r: AGTTGGATTCATCTCACACTGC	91
<b>DMR8</b>	chr4:6149607-6149696	f: TGGAAAGTTTTCAACCTGCTG r: TACAACTTATTTTTCAGACTACATGACC	SYBR
<b>DMR9</b>	chr7:141369180+141369299	f: CTTGTTGACAACTGTAAGGAGGAG r: TGTCGATGCCCAAATACAGA	SYBR
<b>no DMR</b>	chr5:106049748+106049818	f: CAATACCACAGTAAGAGCTGCCTAA r: GGAAGCCCTGAGAGAGCTG	19



ChIP-qPCR primers (Supplemental Fig. S2G)

ChIP Primer	Genomic coordinates (NCBI37/mm9)	Primer sequence	UPL probe
<b>CTRL1 (<i>Gapdh</i>)</b>	chr6:125115169-125115257	f: CCTACGCAGGTCTTGCTGA r: TGACCTTGAGGTCTCCTTGG	10
<b>1</b>	chr13:90028893-90028952	f: GCCTAGCTGCAGTTTCATCA r: CTGACTCCACTGAGGCTGATT	66
<b>2 (=2I, DMR3)</b>	chr17:50250575-50250654	f: AACATTCTGCAGCCCATTC r: ACAACCAGGGCATTGCTTA	6
<b>3</b>	chr12:76803394-76803467	f: CTGGAGCCGTTTCTTCAGG r: ATTTTGTGGTGGGCTTCCTA	62
<b>4</b>	chr12:76803468-76803557	f: TCCGTATCTCCCTCCTAACACT r: CGTGTGTTAGACAATCTAGACGTTG	100
<b>5</b>	chr7:138086947-138087019	f: GTTGCGCAATGAGCTCTCTA r: CACGCTGAGACAAACACTC	27
<b>6</b>	chr11:50192068-50192161	f: CCGCTGTTACGCAATGGT r: AGTTTTAAAAGAAAACAAATTCAGCAG	89
<b>7</b>	chr8:122364548-122364618	f: ATCCAGTCTGTGCGGATT r: GAAGGGAAGACGAGGAGGAA	19
<b>8</b>	chr6:115403104-115403165	f: AGCCAGTGCAGAGTTTAGC r: GGTAGATTTTGGGAGGAAGG	48
<b>9 (=2I, DMR6)</b>	chr1:170292711-170292778	f: GGGACAGGGAGCTACTAGGAA r: TCGCACTTGGCAAGACTCTA	67
<b>10</b>	chr4:97770997-97771069	f: TGGTTTGGACAAGTGCTGTG r: CAGGAGCATGTGCAATAGTTTT	29
<b>11</b>	chr4:57852232+57852354	f: AAATTAAGTTCTGTGACTTTTGACTCC r: GGGGCTGTCCGTAGACATT	17
<b>12 (=2I, DMR7)</b>	chr5:107420675-107420749	f: AAATTAAGTTCTGTGACTTTTGACTCC r: AGTTGGATTCATCTCACACTGC	91

## MS-qPCR primers (Supplemental Fig. S2C)

Note: Primers are not identical with Fig. 2I

Primer	Genomic coordinates (NCBI37/mm9)	Primer sequence (forward and reverse)	UPL probe
<b>Gapdh</b>	chr6:125115169-125115257	f: CCTACGCAGGTCTTGCTGA r: TGACCTTGAGGTCTCCTTGG	10
<b>Peg3</b>	chr7:6683069-6683210	f: AGTGGACCCACACTGAACC r: GAGAAGCGGAGAGATGTCCA	26
<b>DMR1</b>	chr2:173091915-173092050	f: TTCCTCCTATGGCTGTGACC r: AAGGCGTGAATCATTATTGGT	33
<b>DMR2</b>	chr18:23940746-23940854	f: TTCTTTGTTTAACTTGTCATCTAGCC r: GGTTGGGAGACATAAGGACTCA	9
<b>DMR3</b>	chr18:23940753-23940854	f: TTTAACTTGTCATCTAGCCTCAGC r: GGTTGGGAGACATAAGGACTCA	9
<b>DMR4</b>	chr4:105314322-105314417	f: GTTCACCTCTTGAAGCTTTTCTCA r: CAACATGTTTATTTCACATGGAGAGA	55
<b>DMR5</b>	chr16:92449531-92449606	f: TGCGGTAAAAAGTCTCATGC r: ATTCGGAGCGTGTGTCTT	-
<b>DMR6</b>	chr8:49394994-49395067	f: GAAACCCAAGAGGGGAAA r: TCAGTGAAAAGATGTGTTTCGAGA	-
<b>DMR7</b>	chr6:4460009-4460109	f: TGGAAATAATTGTGAAGCAGTCA r: CACCGAAATGTAGCAAAAATG	-
<b>DMR8</b>	chr2:118844243-118844321	f: CGATGAGTGTGTGAGCGAAT r: AGGAACAAGGGTAGCCAAGG	-
<b>DMR9</b>	chrX:166435711-166435776	f: CCCTAGGTAGCGCAGTGAGT r: ACACGGGGTCTCTGTGTCTG	-
<b>DMR10</b>	chr7:13489136-13489248	f: GGAATCCAGCCCTAGCTTTAC r: GCTCTCGCAGTTGGGCTA	42
<b>DMR11</b>	chr11:49624657-49624751	f: TCCCTAGTGTGAGCCTTAGCC r: CACAGCAGCCCTCAAGATAA	102
<b>DMR12</b>	chr19: 38746596-38746995	f: GCAATCCTAACAAAAATACTGAAGTG r: GGCTCTGACACTGTGGTTGA	97
<b>DMR13</b>	chr18:66287008-66287118	f: AAAGCTATGCCTTGAACCAT r: TTCCCATTCAGGGCTGTAAA	-
<b>DMR14</b>	chr5:53794142-53794231	f: TGAGTGTGCTATGTGTCAGCAG r: AGGAAGCTAGTTCTACGAATCCAC	6
<b>DMR15</b>	chr10:99495588-99495662	f: CATCCCTCCAAACGTGTCT r: TCATGATGACTCCACACAGGA	-
<b>DMR16</b>	chr18:23940654-23940729	f: TGGTGGCTACCCAGAGT r: GGCTGGTCTCTTGGGACA	66
<b>DMR17</b>	chrX:166435106-166435188	f: ACACAGCGTGAACGACCAG r: GCCTGAGACGAATCAATGAAA	-
<b>DMR18</b>	chr13:113545830-113545918	f: ACCACGGAGCTGAGTCCTAA r: AGGAATCAGGAGACAACTATGGA	53

## Supplemental References

- Andressoo JO, Weeda G, Wit J de, Mitchell JR, Beems RB, van Steeg H, van der Horst, G. T., Hoeijmakers JH. 2009. An Xpb mouse model for combined xeroderma pigmentosum and cockayne syndrome reveals progeroid features upon further attenuation of DNA repair, *Molecular and cellular biology* **29**: 1276–1290 doi: 10.1128/MCB.01229-08.
- Arizmendi C, Liu S, Croniger C, Poli V, Friedman JE. 1999. The transcription factor CCAAT/enhancer-binding protein beta regulates gluconeogenesis and phosphoenolpyruvate carboxykinase (GTP) gene transcription during diabetes, *The Journal of biological chemistry* **274**: 13033–13040.
- Brack AS, Conboy MJ, Roy S, Lee M, Kuo CJ, Keller C, Rando TA. 2007. Increased Wnt signaling during aging alters muscle stem cell fate and increases fibrosis, *Science* **317**: 807–810 doi: 10.1126/science.1144090.
- Brennan TA, Egan KP, Lindborg CM, Chen Q, Sweetwyne MT, Hankenson KD, Xie SX, Johnson FB, Pignolo RJ. 2014. Mouse models of telomere dysfunction phenocopy skeletal changes found in human age-related osteoporosis, *Disease models & mechanisms* **7**: 583–592 doi: 10.1242/dmm.014928.
- Castilho RM, Squarize CH, Chodosh LA, Williams BO, Gutkind JS. 2009. mTOR mediates Wnt-induced epidermal stem cell exhaustion and aging, *Cell stem cell* **5**: 279–289 doi: 10.1016/j.stem.2009.06.017.
- Chen Q, Liu K, Robinson AR, Clauson CL, Blair HC, Robbins PD, Niedernhofer LJ, Ouyang H. 2013. DNA damage drives accelerated bone aging via an NF-kappaB-dependent mechanism, *Journal of bone and mineral research : the official journal of the American Society for Bone and Mineral Research* **28**: 1214–1228 doi: 10.1002/jbmr.1851.
- Compe E, Drane P, Laurent C, Diderich K, Braun C, Hoeijmakers JH, Egly JM. 2005. Dysregulation of the peroxisome proliferator-activated receptor target genes by XPD mutations, *Molecular and cellular biology* **25**: 6065–6076 doi: 10.1128/MCB.25.14.6065-6076.2005.
- Coppe JP, Patil CK, Rodier F, Krtolica A, Beausejour CM, Parrinello S, Hodgson JG, Chin K, Desprez PY, Campisi J. 2010. A human-like senescence-associated secretory phenotype is conserved in mouse cells dependent on physiological oxygen, *PLoS one* **5**: e9188 doi: 10.1371/journal.pone.0009188.
- Coppe JP, Patil CK, Rodier F, Sun Y, Munoz DP, Goldstein J, Nelson PS, Desprez PY, Campisi J. 2008. Senescence-associated secretory phenotypes reveal cell-nonautonomous functions of oncogenic RAS and the p53 tumor suppressor, *PLoS biology* **6**: 2853–2868 doi: 10.1371/journal.pbio.0060301.
- de Boer J, Andressoo JO, Wit J de, Huijmans J, Beems RB, van Steeg H, Weeda G, van der Horst, G. T., van Leeuwen W, Themmen AP, et al. 2002. Premature aging in mice deficient in DNA repair and transcription, *Science* **296**: 1276–1279 doi: 10.1126/science.1070174.
- de Boer J, Wit J de, van Steeg H, Berg RJ, Morreau H, Visser P, Lehmann AR, Duran M, Hoeijmakers JH, Weeda G. 1998. A mouse model for the basal transcription/DNA repair syndrome trichothiodystrophy, *Molecular cell* **1**: 981–990.
- Dimri GP, Lee X, Basile G, Acosta M, Scott G, Roskelley C, Medrano EE, Linskens M, Rubelj I, Pereira-Smith O, et al. 1995. A biomarker that identifies senescent human cells in culture and in aging skin in vivo, *Proceedings of the National Academy of Sciences of the United States of America* **92**: 9363–9367.
- Harada YN, Shiomi N, Koike M, Ikawa M, Okabe M, Hirota S, Kitamura Y, Kitagawa M, Matsunaga T, Nikaido O, et al. 1999. Postnatal growth failure, short life span, and early onset of cellular senescence and subsequent immortalization in mice lacking the xeroderma pigmentosum group G gene, *Molecular and cellular biology* **19**: 2366–2372.

- Hemmerlyckx B, Hoylaerts MF, Lijnen HR. 2012. Effect of premature aging on murine adipose tissue, *Experimental gerontology* **47**: 256–262 doi: 10.1016/j.exger.2012.01.001.
- Huggins CJ, Malik R, Lee S, Salotti J, Thomas S, Martin N, Quinones OA, Alvord WG, Olanich ME, Keller JR, et al. 2013. C/EBPgamma suppresses senescence and inflammatory gene expression by heterodimerizing with C/EBPbeta, *Molecular and cellular biology* **33**: 3242–3258 doi: 10.1128/MCB.01674-12.
- Inoue Y, Inoue J, Lambert G, Yim SH, Gonzalez FJ. 2004. Disruption of hepatic C/EBPalpha results in impaired glucose tolerance and age-dependent hepatosteatosis, *The Journal of biological chemistry* **279**: 44740–44748 doi: 10.1074/jbc.M405177200.
- Jaskelioff M, Muller FL, Paik JH, Thomas E, Jiang S, Adams AC, Sahin E, Kost-Alimova M, Protopopov A, Cadinanos J, et al. 2011. Telomerase reactivation reverses tissue degeneration in aged telomerase-deficient mice, *Nature* **469**: 102–106 doi: 10.1038/nature09603.
- Karakasilioti I, Kamileri I, Chatzinikolaou G, Kosteas T, Vergadi E, Robinson AR, Tsamardinos I, Rozgaja TA, Siakouli S, Tsatsanis C, et al. 2013. DNA damage triggers a chronic autoinflammatory response, leading to fat depletion in NER progeria, *Cell Metab* **18**: 403–415 doi: 10.1016/j.cmet.2013.08.011.
- Kuro-o M, Matsumura Y, Aizawa H, Kawaguchi H, Suga T, Utsugi T, Ohyama Y, Kurabayashi M, Kaname T, Kume E, et al. 1997. Mutation of the mouse klotho gene leads to a syndrome resembling ageing, *Nature* **390**: 45–51 doi: 10.1038/36285.
- Liu H, Fergusson MM, Castilho RM, Liu J, Cao L, Chen J, Malide D, Rovira, II, Schimel D, Kuo CJ, et al. 2007. Augmented Wnt signaling in a mammalian model of accelerated aging, *Science* **317**: 803–806 doi: 10.1126/science.1143578.
- Liu S, Croniger C, Arizmendi C, Harada-Shiba M, Ren J, Poli V, Hanson RW, Friedman JE. 1999. Hypoglycemia and impaired hepatic glucose production in mice with a deletion of the C/EBPbeta gene, *The Journal of clinical investigation* **103**: 207–213 doi: 10.1172/JCI4243.
- Lumeng CN, Liu J, Geletka L, Delaney C, Delproposto J, Desai A, Oatmen K, Martinez-Santibanez G, Julius A, Garg S, et al. 2011. Aging is associated with an increase in T cells and inflammatory macrophages in visceral adipose tissue, *Journal of immunology* **187**: 6208–6216 doi: 10.4049/jimmunol.1102188.
- McWhir J, Selfridge J, Harrison DJ, Squires S, Melton DW. 1993. Mice with DNA repair gene (ERCC-1) deficiency have elevated levels of p53, liver nuclear abnormalities and die before weaning, *Nature genetics* **5**: 217–224 doi: 10.1038/ng1193-217.
- Moore SG, Dawson KL. 1990. Red and yellow marrow in the femur. age-related changes in appearance at MR imaging, *Radiology* **175**: 219–223.
- Mounkes LC, Kozlov S, Hernandez L, Sullivan T, Stewart CL. 2003. A progeroid syndrome in mice is caused by defects in A-type lamins, *Nature* **423**: 298–301 doi: 10.1038/nature01631.
- Niedernhofer LJ, Garinis GA, Raams A, Lalai AS, Robinson AR, Appeldoorn E, Odijk H, Oostendorp R, Ahmad A, van Leeuwen W, et al. 2006. A new progeroid syndrome reveals that genotoxic stress suppresses the somatotroph axis, *Nature* **444**: 1038–1043 doi: 10.1038/nature05456.
- Peinado JR, Quiros PM, Pulido MR, Marino G, Martinez-Chantar ML, Vazquez-Martinez R, Freije JM, Lopez-Otin C, Malagon MM. 2011. Proteomic profiling of adipose tissue from Zmpste24<sup>-/-</sup> mice, a model of lipodystrophy and premature aging, reveals major changes in mitochondrial function and vimentin processing, *Molecular & cellular proteomics : MCP* **10**: M111 008094 doi: 10.1074/mcp.M111.008094.

- Pendas AM, Zhou Z, Cadinanos J, Freije JM, Wang J, Hultenby K, Astudillo A, Wernerson A, Rodriguez F, Tryggvason K, et al. 2002. Defective prelamin A processing and muscular and adipocyte alterations in Zmpste24 metalloproteinase-deficient mice, *Nature genetics* **31**: 94–99 doi: 10.1038/ng871.
- Prasher JM, Lalai AS, Heijmans-Antonissen C, Ploemacher RE, Hoeijmakers JH, Touw IP, Niedernhofer LJ. 2005. Reduced hematopoietic reserves in DNA interstrand crosslink repair-deficient Ercc1<sup>-/-</sup> mice, *The EMBO journal* **24**: 861–871 doi: 10.1038/sj.emboj.7600542.
- Rahman SM, Janssen RC, Choudhury M, Baquero KC, Aikens RM, de la Houssaye, B. A., Friedman JE. 2012. CCAAT/Enhancer-binding Protein beta (C/EBP beta) Expression Regulates Dietary-induced Inflammation in Macrophages and Adipose Tissue in Mice, *J Biol Chem* **287**: 34349–34360 doi: 10.1074/jbc.M112.410613.
- Rudolph KL, Chang S, Lee HW, Blasco M, Gottlieb GJ, Greider C, DePinho RA. 1999. Longevity, stress response, and cancer in aging telomerase-deficient mice, *Cell* **96**: 701–712.
- Screpanti I, Romani L, Musiani P, Modesti A, Fattori E, Lazzaro D, Sellitto C, Scarpa S, Bellavia D, Lattanzio G, et al. 1995. Lymphoproliferative disorder and imbalanced T-helper response in C/EBP beta-deficient mice, *The EMBO journal* **14**: 1932–1941.
- Siersbaek R, Rabiee A, Nielsen R, Sidoli S, Traynor S, Loft A, La Cour Poulsen L, Rogowska-Wrzęsinska A, Jensen ON, Mandrup S. 2014. Transcription factor cooperativity in early adipogenic hotspots and super-enhancers, *Cell reports* **7**: 1443–1455 doi: 10.1016/j.celrep.2014.04.042.
- Smink JJ, Begay V, Schoenmaker T, Sterneck E, Vries TJ de, Leutz A. 2009. Transcription factor C/EBPbeta isoform ratio regulates osteoclastogenesis through MafB, *The EMBO journal* **28**: 1769–1781 doi: 10.1038/emboj.2009.127.
- Staiger J, Lueben MJ, Berrigan D, Malik R, Perkins SN, Hursting SD, Johnson PF. 2009. C/EBP beta regulates body composition, energy balance-related hormones and tumor growth, *Carcinogenesis* **30**: 832–840 doi: 10.1093/carcin/bgn273.
- Sterneck E, Tessarollo L, Johnson PF. 1997. An essential role for C/EBP beta in female reproduction, *Gene Dev* **11**: 2153–2162 doi: 10.1101/gad.11.17.2153.
- Tanaka T, Yoshida N, Kishimoto T, Akira S. 1997. Defective adipocyte differentiation in mice lacking the C/EBPbeta and/or C/EBPdelta gene, *The EMBO journal* **16**: 7432–7443 doi: 10.1093/emboj/16.24.7432.
- Trifunovic A, Wredenberg A, Falkenberg M, Spelbrink JN, Rovio AT, Bruder CE, Bohlooly YM, Gidlof S, Oldfors A, Wibom R, et al. 2004. Premature ageing in mice expressing defective mitochondrial DNA polymerase, *Nature* **429**: 417–423 doi: 10.1038/nature02517.
- van de Ven M, Andressoo JO, Holcomb VB, Lindern M von, Jong WM, Zeeuw CI de, Suh Y, Hasty P, Hoeijmakers JH, van der Horst, G. T., et al. 2006. Adaptive stress response in segmental progeria resembles long-lived dwarfism and calorie restriction in mice, *PLoS genetics* **2**: e192 doi: 10.1371/journal.pgen.0020192.
- van der Pluijm I, Garinis GA, Brandt RM, Gorgels TG, Wijnhoven SW, Diderich KE, Wit J de, Mitchell JR, van Oostrom C, Beems R, et al. 2007. Impaired genome maintenance suppresses the growth hormone--insulin-like growth factor 1 axis in mice with Cockayne syndrome, *PLoS biology* **5**: e2 doi: 10.1371/journal.pbio.0050002.
- Vogel H, Lim DS, Karsenty G, Finegold M, Hasty P. 1999. Deletion of Ku86 causes early onset of senescence in mice, *Proceedings of the National Academy of Sciences of the United States of America* **96**: 10770–10775.
- Wang ND, Finegold MJ, Bradley A, Ou CN, Abdelsayed SV, Wilde MD, Taylor LR, Wilson DR, Darlington GJ. 1995. Impaired energy homeostasis in C/EBP alpha knockout mice, *Science* **269**: 1108–1112.

- White RR, Milholland B, Bruin A de, Curran S, Laberge RM, van Steeg H, Campisi J, Maslov AY, Vijg J. 2015. Controlled induction of DNA double-strand breaks in the mouse liver induces features of tissue ageing, *Nature communications* **6**: 6790 doi: 10.1038/ncomms7790.
- Wiehle L, Raddatz G, Musch T, Dawlaty MM, Jaenisch R, Lyko F, Breiling A. 2015. Tet1 and Tet2 Protect DNA Methylation Canyons against Hypermethylation, *Molecular and cellular biology* **36**: 452–461 doi: 10.1128/MCB.00587-15.
- Yue F, Cheng Y, Breschi A, Vierstra J, Wu W, Ryba T, Sandstrom R, Ma Z, Davis C, Pope BD, et al. 2014. A comparative encyclopedia of DNA elements in the mouse genome, *Nature* **515**: 355–364 doi: 10.1038/nature13992.